UVAROVITE IN PODIFORM CHROMITITE: THE MOA–BARACOA OPHIOLITIC MASSIF, CUBA

JOAQUÍN PROENZA

*Departamento de Geología, Instituto Superior Minero Metalúrgico de Moa,
Las Coloradas s/n, 83320 Moa, Cuba and Departament de Cristal•lografia, Mineralogia i Dipòsits Minerals,
Universitat de Barcelona, C/ Martí i Franquès s/n, E-08028 Barcelona, Catalonia, Spain*

JESÚS SOLÉ AND JOAN CARLES MELGAREJO[§]

*Departament de Cristal•lografia, Mineralogia i Dipòsits Minerals, Universitat de Barcelona,
C/ Martí i Franquès s/n, E-08028 Barcelona, Catalonia, Spain*

ABSTRACT

The chromitite pods of the Moa–Baracoa massif, in the eastern ophiolitic belt of Cuba, contain pre-existing gabbro sills. This association is affected by two processes of hydrothermal alteration. The chromitites and the hosting dunites and harzburgites are affected first by regional serpentinization; a second alteration, represented by chloritization accompanied with formation of ferrian chromite, is mainly located in the pods and their immediate vicinity. The altered chromitite pods and enclosed gabbro sills are cross cut by millimeter-wide veins. The vein filling consists of a sequence of clinochlore, uvarovite, chromian clinochlore, rutile, titanite and calcite. Uvarovite also occurs in the vicinity of veins. Uvarovite is concentrically zoned, covering compositions in the uvarovite–grossular solid solution series between Uva_{17} and Uva_{63}; the andradite component is very low. These compositions suggest a complete miscibility along the grossular–uvarovite join at relatively low temperature. On the basis of the mineral sequence and mineral chemistry (major and trace elements), the uvarovite crystals, as well as the vein assemblage, formed by a low-temperature leaching, Ca probably from the gabbro sills, and Cr and Al from the chromite during the formation of ferrian chromite. Cr and Al would have been mobile only at the scale of a pod during this process.

Keywords: uvarovite, zoning, hydrothermal, chromitite, ophiolite, Moa–Baracoa massif, Cuba.

SOMMAIRE

Les lentilles de chromitite du massif de Moa–Baracoa, dans la partie orientale de la ceinture ophiolitique de Cuba, contient des filon-couches de gabbro. Cette association a subi les effets de deux stades d'altération hydrothermale. Les lentilles de chromitite et la dunite et la harzburgite encaissantes ont d'abord subi l'influence d'une serpentinisation régionale. Une deuxième altération a causé une chloritisation et la formation de chromite ferrique, surtout dans les lentilles et leurs environs. Les lentilles de chromitite altérées et les filon-couches de gabbro sont recoupés par des veines millimétriques tapissées de clinochlore, uvarovite, clinochlore chromifère, rutile, titanite et calcite. L'uvarovite se trouve aussi tout près des veines. Les cristaux d'uvarovite montrent une zonation concentrique, et les compositions s'étalent entre uvarovite Uva_{63} et grossulaire Uva_{17}. La teneur en andradite est très faible. Ces compositions font penser qu'il y a une miscibilité complète entre grossulaire et uvarovite à température relativement faible. A la lumière de la séquence paragénétique et de la composition des minéraux (éléments majeurs et traces), les cristaux d'uvarovite, ainsi que l'assemblage des veines, se sont formés par lessivage à faible température, le calcium venant probablement des filon-couches de gabbro, et le Cr et Al contribués par la chromite lors de la formation de la chromite ferrique. Le chrome et l'aluminium n'auraient été mobiles qu'à l'échelle d'une lentille pendant ce processus.

(Traduit par la Rédaction)

Mots-clés: uvarovite, zonation, altération hydrothermale, chromitite, ophiolite, massif de Moa–Baracoa, Cuba.

[§]   *E-mail address*: joanc@natura.geo.ub.es

INTRODUCTION

The uvarovite end-member of the garnet group, $Ca_3Cr_2(SiO_4)_3$, has not yet been found in nature. Natural uvarovitic garnet typically contains significant amounts of both grossular and andradite components. Such compositions have been recorded in diverse geological settings: chromitites associated with basic and ultrabasic rocks (Chakraborty 1968, Jan *et al.* 1984, Graham *et al.* 1996, Proenza & Melgarejo 1996, Melcher *et al.* 1997), rodingites (Mogessie & Rammlmair 1994), skarns (von Knorring *et al.* 1986, Pan & Fleet 1989), and kimberlites (Meyer & Boyd 1972, Sobolev *et al.* 1973). The range of environments in which it is found suggests a broad field of stability (Kalamarides & Berg 1988).

Our aim in this paper is to provide new chemical and structural data on this important garnet, and to describe its mineral association and petrological significance in the Mayarí–Baracoa ophiolitic belt, Cuba.

GEOLOGICAL SETTING

The northern part of the island of Cuba is characterized by a 1000-km-long Upper Jurassic – Lower Cretaceous ophiolitic belt (Iturralde-Vinent 1996). The eastern part, the Mayarí–Baracoa ophiolitic belt (Fig. 1), is 170 km long, 10 to 20 km wide, and comprises two allochthonous massifs: Mayarí–Cristal and Moa–Baracoa. Both massifs contain abundant podiform deposits of chromitite (Thayer 1942, Guild 1947, Murashko & Lavandero 1989, Proenza *et al.* 1997a, 1999, Proenza 1998). The Mayarí–Cristal massif, the

western part of the Mayarí–Baracoa belt, is mainly composed of serpentinized ultrabasic rocks (harzburgite and interlayered harzburgite and dunite), with microgabbros and a diabase dike complex overlying the unit (Iturralde-Vinent 1996). Chromitite pods occur within the dunite; the chromite is relatively Cr-rich, with $Cr/(Cr + Al) \approx$ 0.75 (metallurgical grade).

The Moa–Baracoa massif is also mainly composed of serpentinized ultrabasic rocks; harzburgite grades upward to harzburgite and dunite. In the uppermost part of the mantle section, sills and dikes of gabbro are common; this suite is covered by a crustal section comprising, from bottom to top, banded gabbro, isotropic gabbro, gabbro with diabase dikes and, finally, basalt and chert. The chromitite pods, commonly with dunitic envelopes, occur in the uppermost part of the mantle–crust transition zone (MTZ). Many chromitites enclose and replace the older gabbro sills parallel to the elongation of the pods (Fig. 2). This feature is typical of most chromite deposits of the Moa–Baracoa district (Proenza *et al.* 1997a, 1999), as well as of other districts in central Cuba (Flint *et al.* 1948) and at Coto in the Zambales ophiolite in Philippines (Leblanc & Violette 1983). These chromitites are made up of Al-rich chromite or chromian hercynite, with $Cr/(Cr+Al) \approx 0.45$ (refractory grade).

Uvarovitic garnet related to chromitites has been found only in the Moa–Baracoa massif (Guild 1947, Kenarev 1966, Lewis *et al.* 1994, Proenza & Melgarejo 1996). Consequently, the Moa–Baracoa chromite ores will be described with greater detail. However, their absence in Mayarí–Cristal massif has genetic implications as discussed later.

FIG. 1.   Geological sketch of the northwestern Caribbean ophiolites (modified from Wadge *et al.* 1984).
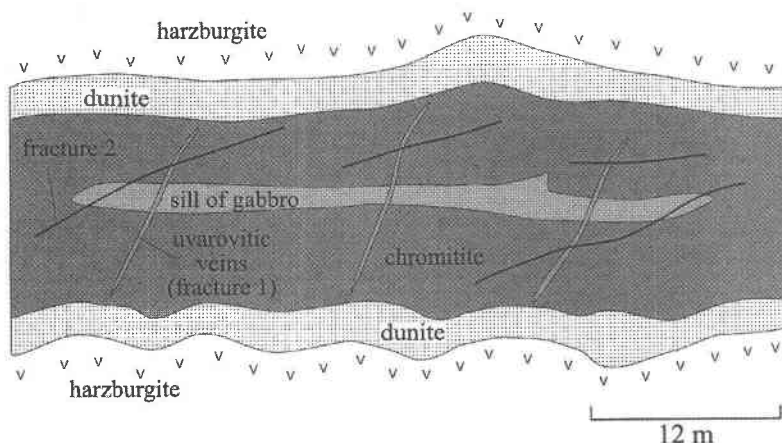
FIG. 2. Schematic sketch of the chromite bodies, showing the gabbro sills and the two sets of veins.

THE CHROMITE ORES IN MOA–BARACOA AND THE UVAROVITE OCCURRENCES

A first stage in the formation of the chromitite pods involved the magmatic processes that produced the deposit. Primary mineralization is formed by chromite plus interstitial olivine and, as small inclusions in chromite, minor amounts of clinopyroxene, amphibole and plagioclase. This association replaced the enclosed pre-chromitite gabbro sills, as well as the hosting dunite and harzburgite (Proenza et al. 1997a, 1999, Proenza 1998).

The texture of the chromitite is massive, grading in some deposits to disseminated, and displays pull-apart fractures. This type of fracture is very common in podiform deposits of chromite, and it is visible in hand samples as well as on the scale of the deposit (i.e., Leblanc & Nicolas 1992).

Subsolidus hydrothermal processes produced secondary minerals that widely replaced the above mineral association. Two main stages of alteration can be distinguished. The first stage was regional, and affected the chromitite pods and the host rocks (dunite and harzburgite), replacing the olivine grains by an assemblage of serpentine plus magnetite. The second stage took place largely in the chromitite pods and their vicinity, and comprises chromite alteration into ferrian chromite ("ferritchromit"), coupled with replacement of serpentine by Cr-poor clinochlore (clinochlore-I, Proenza et al. 1997b). This type of alteration is poorly developed in harzburgite or dunite occurring far from the pods, and is restricted to a millimeter scale in the vicinity of the small grains of accessory chromian spinel.

The chromitite bodies of the Moa–Baracoa massif are cross-cut by two sets of mineralized joints (Fig. 3). Uvarovitic garnet appears only within the first set.

Uvarovite appears also in an alteration zone, up to several centimeters in width, that replaces the hosting chromitite along these fractures. In this case, the chromite grains are partly corroded and replaced by uvarovite, and the replacement of chromite progresses along the grain boundaries and the pull-apart fractures.
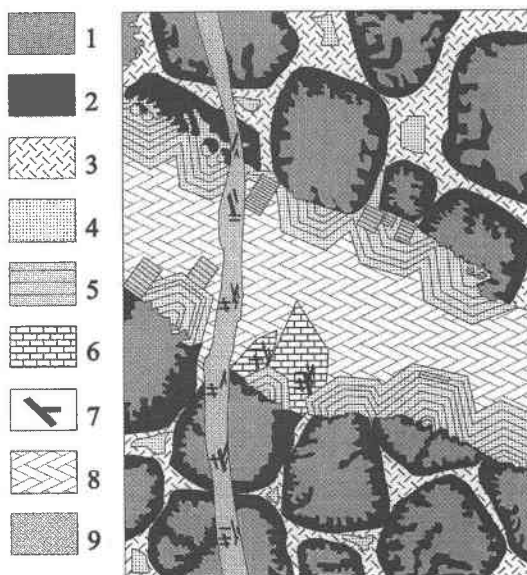

FIG. 3. Schematic cross-section of the garnet-bearing veins. Symbols: 1) chromite, 2) ferrian chromite, 3) clinochlore-I, 4) uvarovite, 5) clinochlore-II (chromian clinochlore), 6) titanite, 7) rutile, 8) calcite, and 9) clinochlore-III.

In many cases, the uvarovite crystals from these zones includes relics of chromite.

In contrast, the vein-type mineralization has a drusy character, and represents a typical example of the filling of open spaces from a hydrothermal solution. The vein mineralization can fill small joints up to 1 cm thick (Fig. 4), or small zones of breccia. Both types of mineralization are limited to the interior of the chromitite bodies. Despite the fact that the contacts of these fractures with chromitite are sharp, the chromite of the walls and of the breccia fragments also displays signs of replacement at a microscopic scale by the infilling minerals. The paragenetic sequence of these veins (Fig. 5) begins with the crystallization of a first generation of Cr-rich clinochlore (clinochlore II, in euhedral columnar crystals, up to 200 μm in size) and zoned euhedral crystals of uvarovite developed on the walls of the fractures (Figs. 3, 6, 7). The uvarovitic garnet displays an emerald-green color, with a vitreous luster. The crystals are rhombic dodecahedra {110}, and are generally between 0.1 and 0.7 mm in diameter. Zoning is visible with the naked eye (variable hues of green, from emerald green to pale grass green). Under the polarizing microscope, zoning is also distinguished by changes in birefringence (up to 0.006); complex sector twinning also is present (Fig. 8). The pattern of zoning is similar to the growth zoning of grossular–andradite garnet in hydrothermal systems described by Jamtveit *et al.*

FIG. 4.   Detail of the uvarovite veins in hand sample. Massive chromitite (black) is cut by millimetric veins of uvarovite (dark green). Calcite crystals (white) occur in the central part of these veins. The interstitial areas between chromite grains are filled by clinochlore (grey).

(1995). In many cases, small inclusions of clinochlore lie parallel to the zones in the garnet, and inclusions of chromite (strongly corroded) may occur, especially close to the contact with the chromitite.

Rutile appears simultaneously with uvarovite and develops groups of euhedral columnar crystals, twinned on {011} (sagenitic variety) up to 500 μm long. It is subsequently overgrown (and, in part, replaced) by euhedral titanite (greenish, up to 4 mm long).

	Primary mineralization	Alteration		Fractures	
		serpentinitization	chloritization	first generation	second generation
Chromite	▬▬▬				
Olivine	▬▬▬				
Clinopyroxene	▬				
Plagioclase	▬				
Serpentine		▬▬▬			
Magnetite		—			
"Ferritchromit"			▬▬		—
Clinochlore-I			▬▬		
Clinochlore-II				▬▬	
Rutile				—	—
Uvarovite				▬▬	
Titanite				▬▬	
Calcite				▬▬	
Clinochlore-III					▬▬

FIG. 5.   Sequence of crystallization in the chromite pods and veins. Width of the bars indicates the relative abundance of minerals in each episode. Solid bars are used where the temporal extension of a given mineral can be well established; a dash is used in the absence of definitive arguments.
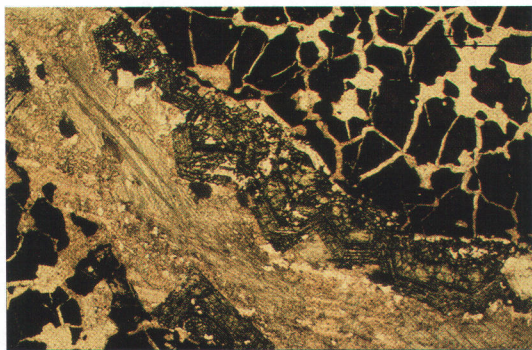
FIG. 6. Photomicrograph of a uvarovite vein. The host pod of chromitite is largely composed of chromite (black). The original interstitial olivine grains were replaced by clinochlore (clear). Euhedral, zoned, uvarovite crystals grew on the wall of the vein, and calcite crystals fill the rest of pore space in the vein. Plane-polarized light. Width of photo 5.6 mm.
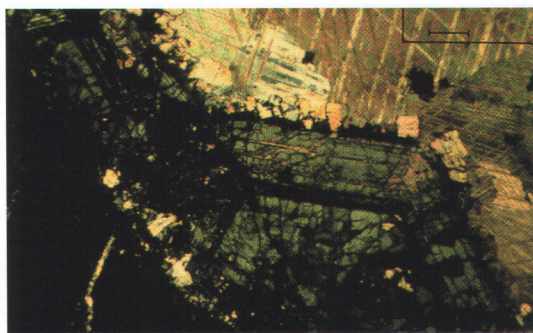

FIG. 7. Detail of the uvarovite veins. The garnet displays oscillatory zoning and is covered by euhedral crystals of clinochlore and late calcite. Plane-polarized light, crossed polars. Width of photo 2.8 mm.
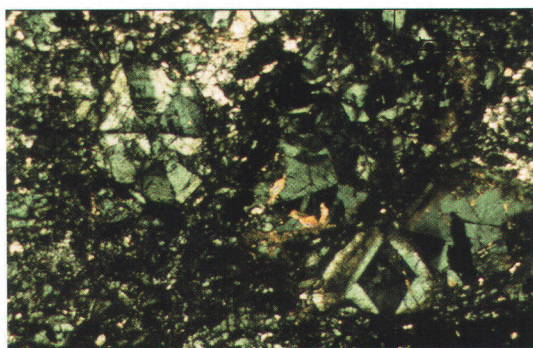

FIG. 8. Complex zoning and rhombic dodecahedral twinning in uvarovite crystals from the veins. Plane-polarized light. Crossed polars. Width of photo 1.4 mm.

Fine-grained Cr-rich clinochlore II was formed later, together with anhedral calcite. These minerals fill the open space of the druses and replace the above minerals. A later generation of titanite plus radial aggregates of clinochlore (both fine-grained) grew on the cleavage planes of calcite.

A second generation of fractures (Figs. 2, 3, 5) crosscuts the earlier fractures at steep angles. The infilling veins are less than 100 μm in width, and all the minerals (clinochlore and sagenitic rutile) are cryptocrystalline. This clinochlore (clinochlore III) is Cr-free. The contact with the uvarovite veins is sharp, and there is no evidence of replacement of the uvarovite assemblage.

ANALYTICAL METHODS

Minerals in thirty polished thin sections were analyzed using a four-channel CAMECA SX–50 electron microprobe. The acceleration potential was 15 kV, the sample current, 15 nA, and the beam diameter, 2 μm. The duration of the counts was 10 s. Concentrations of Mn and Cr were measured with a LiF crystal; those of Si, Al and Mg were measured with a TAP crystal, and Ca and Ti with a PET crystal. The $K\alpha$ lines were used in all cases. The following standards were used: orthoclase (Si and Al), rutile (Ti), Fe_2O_3 (Fe), rhodonite (Mn), periclase (Mg), Cr_2O_3 (Cr) and wollastonite (Ca). More than 200 analyses of garnet were made.

The concentration of trace elements was measured with a Perkin Elmer Elan 6000 inductively coupled plasma – mass spectrometer (ICP–MS) using Rh as internal standard. One sample of uvarovitic garnet was hand-picked from a vein cutting a sample of chromitite. Special attention was made in order to select the most homogeneous, transparent and inclusion-free volume of garnet attainable. Microscopic and X-ray-diffraction analyses do not show any impurities. The garnet was crushed in a corundum mortar and desiccated for 12 hours at 110°C. About 100 mg of sample were weighed and placed in Teflon vessels. A duplicate analysis and four blanks were prepared. The samples were dissolved in a hot mixture of 2 mL of $HClO_4$ plus 10 mL of HF until evaporation. This procedure was repeated three times to ensure complete dissolution of the mineral. The measured blanks were below 0.01 ppb in the final 1:250 dilution for Cs, Pr, Sm, Eu, Gd, Tb, Dy, Ho, Er, Tm, Yb, Lu, Th and U, below 0.1 ppb for Co, Ga, Nb, and Nd, between 0.1 and 0.2 ppb for Li, Rb and La, below 1 ppb for Sr, Sn, Hf and Ce, and between 1 and 5 ppb for V, Ni, Cu, Ba and Pb.

An aliquot of the sample analyzed by ICP–MS was used to determine the unit-cell parameter by powder X-ray diffraction. The X-ray diffraction pattern was obtained with a Siemens DX–500 diffractometer, in step-scan mode between 10° and 150°2θ. The step size was of 0.020°, and the counting time, 20 seconds, with a total of 7000 measured points. No internal standard was used because the zero-point also was refined. Cell

parameters were determined using the Rietveld method implemented in the FULLPROF program (Rodríguez-Carvajal 1990). The pattern was refined in space group *Ia3d* (Deer *et al.* 1992), but it is important to note that other cubic space groups also are possible for garnet compositions of this type (*i.e.*, Pinet & Schmidt 1993).

MINERAL CHEMISTRY

Major elements

A representative set of microprobe results is given in Table 1. Their compositions cover a large interval of uvarovite–grossular solid solution, with a very low andradite component (Fig. 9). Garnet present as interstitial grains from the alteration zone of chromitite has the same composition as garnet from the veins. The Fe content is low, and charge-balance considerations suggest that all the iron is trivalent; nevertheless, it is difficult to assign the correct charge to such small amounts of Fe. The Ti was assigned to occupy octahedral positions. The amounts of V, Mn and Mg are very low or below the detection limit, and these garnet compositions can therefore be represented essentially as solid solutions of the binary series grossular–uvarovite, with 17 to 63 mol.% uvarovite.

TABLE 1. REPRESENTATIVE RESULTS OF
ELECTRON-MICROPROBE ANALYSES OF UVAROVITIC GARNET,
MOA–BARACOA MASSIF, CUBA

Sample	1	2	3	4	5	6	7	8
SiO_2 (wt.%)	38.67	38.60	38.85	37.81	37.49	37.73	37.64	38.03
TiO_2	0.44	0.83	0.47	0.95	3.14	1.57	1.93	2.08
Al_2O_3	15.90	15.34	13.46	10.08	6.79	12.07	9.26	8.62
V_2O_3	0.13	0.26	0.18	0.23	0.72	0.19	0.38	0.37
Cr_2O_3	7.28	8.87	10.39	15.01	16.87	11.78	15.85	16.22
Fe_2O_3	0.69	0.20	0.42	0.38	0.75	0.37	0.34	0.30
CaO	36.21	36.05	35.91	35.66	34.60	35.57	35.06	34.91
Total	99.32	100.14	99.69	100.11	100.36	99.28	100.47	100.52

Structural formula based on 8 cations

Si (apfu)	3.01	2.99	3.04	3.00	3.02	2.99	2.99	3.03
Ti	0.03	0.05	0.03	0.06	0.19	0.09	0.12	0.13
Al	1.46	1.40	1.24	0.94	0.64	1.13	0.87	0.81
V	0.01	0.02	0.01	0.01	0.05	0.01	0.02	0.02
Cr	0.45	0.54	0.64	0.94	1.07	0.74	1.00	1.02
Fe	0.04	0.01	0.02	0.02	0.05	0.02	0.02	0.02
Ca	3.02	2.99	3.01	3.03	2.98	3.02	2.98	2.98
Uva	22.92	27.55	33.46	49.01	59.33	38.85	52.20	54.57
Grs	74.59	71.05	64.64	49.07	35.59	59.35	45.47	43.21
Adr	2.07	0.59	1.30	1.17	2.52	1.15	1.08	0.97
Go	0.42	0.81	0.60	0.76	2.55	0.65	1.26	1.25

1, 2, 3, 4 and 5 fracture-filling uvarovite
6, 7 and 8 disseminated uvarovite grains close to the veins in chromitite
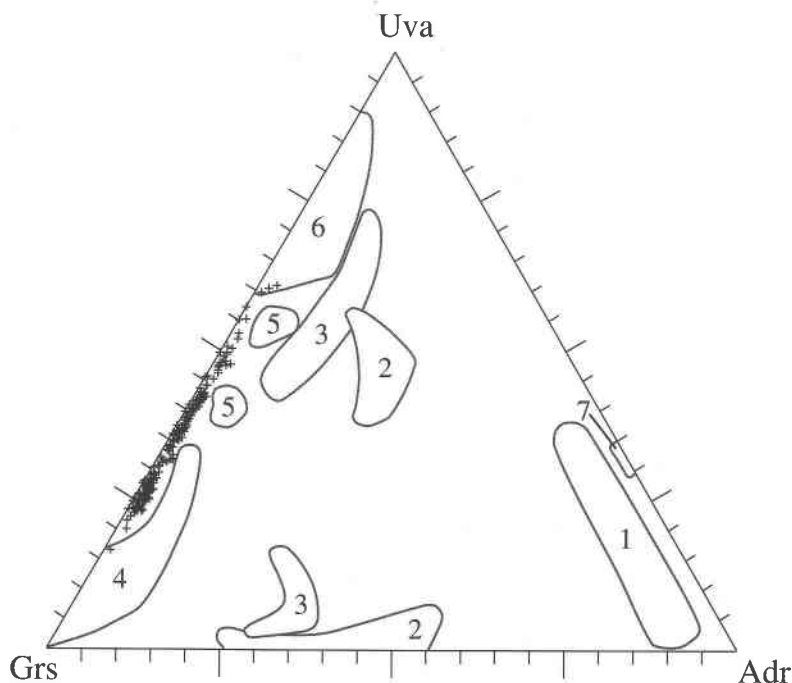End-members molecules calculated after Rickwood (1968)

FIG. 9. Plot of compositions of chromian garnet from the Moa–Baracoa Massif, Cuba, in terms of mol.%, compared to literature data. 1) Reaume Township (Duke & Bonardi 1982), 2) Labrador (Kalamarides & Berg 1988), 3) White River (Pan & Fleet 1989), 4) various localities in Canada (Dunn 1978), 5) Luikonlahti (von Knorring *et al.* 1986), 6) Outukumpu (von Knorring *et al.* 1986), 7) Jijal Complex, Pakistan (Jan *et al.* 1984).

Infrared-absorption and Raman analysis of the garnet was performed on two samples to check for the presence of structurally bound OH. The results were not conclusive with IR, but the Raman spectra shows two bands that may correspond to a very small amount of H_2O. On the other hand, the chemical compositions obtained by electron microprobe agree with those expected of anhydrous garnet, because the tetrahedrally coordinated position is nearly always completely filled with Si.

The zoning is oscillatory, as is easily detected by variations in hues of green. These variations in color reflect variations in the Al:Cr ratio, *i.e.*, the proportion of uvarovite and grossular components (Fig. 10). This kind of zoning is common in chromian garnet (Jan *et al.* 1984). The Cr-rich zones are also the richest in Ti and V. A comparable Cr–Ti correlation has also been observed in the chromian andradite from Reaume Township, Ontario (Duke & Bonardi 1982).

Some differences in Cr content exist among the three generations of chlorite. The early-formed chlorite does not contain Cr (Table 2). It can be classified as clinochlore, after Hey (1954). The second generation of chlorite, which overgrows uvarovite, has Cr contents between 2.5 and 7.5 wt% Cr_2O_3, and is classified as chromian chlinoclore (Table 2). The third generation is again Cr-free. In all three generations, Fe content is very low, and nickel values are lower than 0.2 wt% NiO, with an average as low as 0.05%. Rutile crystals are of end-member composition (Table 2). Titanite contains 39% TiO_2 and 10% Al_2O_3, with variable amounts of Cr, up to 1.4% Cr_2O_3.

TABLE 2. REPRESENTATIVE RESULTS OF ELECTRON-MICROPROBE ANALYSES OF CLINOCHLORE, CHROMIAN CLINOCHLORE, TITANITE AND RUTILE, MOA–BARACOA MASSIF, CUBA

Sample	1	2	3	4	5	6	7	8
SiO_2 (wt.%)	31.76	32.14	27.92	26.81	31.40	30.95	-	-
TiO_2	0.01	0.02	0.00	0.00	39.13	38.52	99.77	99.42
Ta_2O_5	-	-	-	-	-	-	0.00	0.02
Nb_2O_5	-	-	-	-	-	-	0.07	0.00
Al_2O_3	18.32	17.96	20.20	20.50	0.82	0.63	0.11	0.16
Cr_2O_3	0.06	0.07	5.78	7.05	0.34	1.38	0.08	0.03
MgO	35.94	35.88	31.13	30.20	0.00	0.01	0.00	0.03
CaO	0.01	0.03	0.00	0.00	28.55	28.16	0.03	0.00
MnO	0.00	0.02	0.00	0.00	0.00	0.00	0.00	0.07
FeO	0.59	0.80	1.78	1.81	0.00	0.00	-	-
Fe_2O_3	-	-	-	-	-	-	0.00	0.06
NiO	0.09	0.01	0.22	0.19	-	-	-	-
Na_2O	0.02	0.00	0.03	0.03	-	-	-	-
K_2O	0.01	0.00	0.03	0.02	-	-	-	-
H_2O	12.87	12.88	12.55	12.42	-	-	-	-
Total	99.68	99.81	99.64	99.02	100.25	99.65	99.62	99.79
Si (apfu)	5.92	5.99	5.34	5.18	1.02	1.01	-	-
^{IV}Al	2.08	2.01	2.66	2.82	-	-	-	-
^{VI}Al	1.95	1.93	1.89	1.85	0.03	0.02	0.00	0.00
Ti	0.00	0.00	0.00	0.00	0.95	0.95	1.00	1.00
Ta	-	-	-	-	-	-	0.00	0.00
Nb	-	-	-	-	-	-	0.00	0.00
Cr	0.01	0.01	0.87	1.08	0.01	0.04	0.00	0.00
Mg	9.99	9.96	8.87	8.69	0.00	0.00	0.00	0.00
Ca	0.00	0.01	0.00	0.00	0.99	0.99	0.00	0.00
Mn	0.00	0.00	0.00	0.00	0.00	0.00	0.00	0.00
Fe^{2+}	0.09	0.12	0.28	0.29	0.00	0.00	-	-
Fe^{3+}	-	-	-	-	-	-	0.00	0.00
Ni	0.01	0.00	0.03	0.03	-	-	-	-
Na	0.01	0.00	0.01	0.01	-	-	-	-
K	0.00	0.00	0.01	0.00	-	-	-	-

1 and 2: clinochlore (cations calculated on the basis of 28 O)
3 and 4: chromian clinochlore (cations calculated on the basis of 28 O)
5 and 6: titanite (cations calculated on the basis of 3 cat.)
7 and 8: rutile (cations calculated on the basis of 2 O)
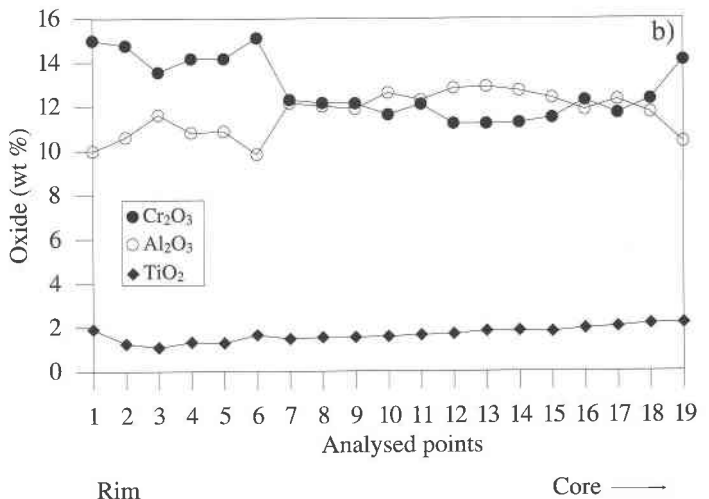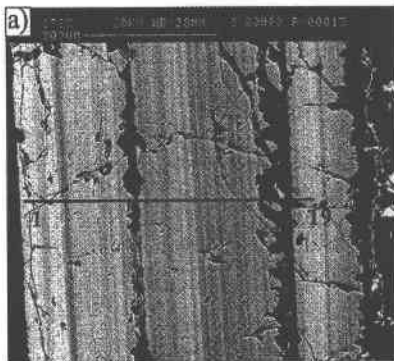

FIG. 10. a) Back-scattered-electron (BSE) image of oscillatory zoning in uvarovite. The line indicates the profile of the crystal analyzed. b) Profile of electron-microprobe data along the line 1–19.

Trace elements

One sample of garnet was analyzed for 31 trace elements by ICP–MS. As far as we know, quantitative data of this type have not been published before. As shown in Table 3, the Moa–Baracoa uvarovite has no detectable amounts of Pb and Ce, a few ppm of Li, Co, Cu, Ga, Rb, Sr, Nb, Sn, Cs, Ba, Hf, Ta, Th and U, and 200 ppm of Ni. The V contents (1000 ppm) is similar to the concentration obtained by electron microprobe. Lanthanide contents are relatively low, not far from being chondritic (Fig. 11).

Compared with the semiquantitative data of Wan & Yeh (1984), the levels of Ni, Cu, Nb, Sn, Ba and Pb are of a similar order of magnitude, but levels of Co, Sr and La are lower in the uvarovite from Moa. The lanthanum content reported by Wan & Yeh (1984) is probably too high because it implies a concentration of lanthanides ten thousand times the chondritic values, which is questionable in such garnet.

DETERMINATION OF THE CELL PARAMETER

We obtained a cell parameter *a* of 11.922 Å using all reflections. This value is a weighed average of the different values of the cell parameter in this slightly zoned garnet. It can be compared to values given by Deer *et al.* (1992) for the end-member garnets. If we assume a linear relationship between cell parameter and composition in the solid solution uvarovite–grossular, and neglect the small andradite component, the cell parameter obtained is equivalent to an average composition of $Uva_{47}Grs_{53}$.

DISCUSSION AND CONCLUSIONS

The garnet-bearing veins are confined to the interior of the chromitite bodies. These veins can be interpreted to be the response to deformation of a rigid body (the chromitites) enclosed by more ductile rocks (the serpentinites). Their formation took place well after the serpentinization process, as is suggested by Bamba (1984) for some alpine podiform deposits of chromite in Turkey.

The textures of the idiomorphic crystals, as well as their position in the veins, indicate that they formed from a hydrothermal fluid in an open space, along fractures. The mineral association points to a formation by a low-temperature hydrothermal process. The existence of a pure Fe-poor clinochlore that cocrystallized with uvarovite in the veins suggests the possibility to estimate the temperatures of formation of this assemblage using chlorite geothermometry. The first generation of clinochlore yields a low temperature, about 180–190°C, using the geothermometer of Hillier & Velde (1991), and 230–240°C using the geothermometer of Kranidiotis
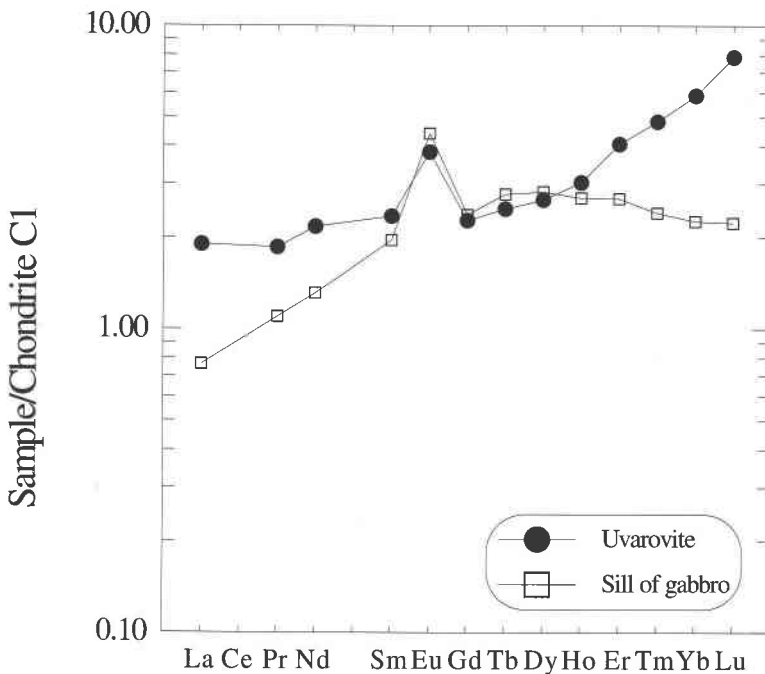

FIG. 11.   Plot of the *REE* data normalized to chondrite for both uvarovite and gabbro sill.

TABLE 3. TRACE-ELEMENT CONCENTRATIONS IN UVAROVITE
FROM THE MOA-BARACOA MASSIF, CUBA

Li	51	Sn	0.3	La	0.451
V	1060	Cs	0.11	Ce	n.d.
Co	2.6	Ba	0.6	Pr	0.177
Ni	238	Hf	12.7	Nd	1.017
Cu	15	Ta	0.02	Sm	0.360
Ga	4.0	Pb	n.d.	Eu	0.222
Rb	0.3	Th	0.09	Gd	0.468
Sr	1.0	U	0.4	Tb	0.093
Nb	0.1			Dy	0.677
				Ho	0.172
				Er	0.673
				Tm	0.123
				Yb	0.999
				Lu	0.200

Analysis by ICP-MS. n.d.: not detected. All values are in ppm.

& MacLean (1987). The estimated temperatures for the second generation of clinochlore (which is associated with uvarovite) are 280–300°C using the first geothermometer. The second yield higher temperatures, about 340–370°C. Therefore, the significant increase in the Cr content of the clinochlore of the second generation results in unrealistically higher temperatures than those of the first generation. The temperatures obtained using both geothermometers in the Cr-free clinochlore of the first generation, however, are in the range of those obtained by Christidis *et al.* (1998) for chlorite formation in the Vourinos ophiolitic complex in Greece.

The complex zoning surfaces of the Moa–Baracoa garnet do not seem to be linked to dissolution processes, but rather to growth. Moreover, their formation at a very low temperature prevents solid-state diffusion as an effective mechanism to explain this zoning (Shore & Fowler 1996). As stated by Jamtveit *et al.* (1995), in ugrandite-type garnet in skarns, the compositions and morphological properties of a hydrothermal mineral are controlled by: a) bulk composition of fluid, b) local transport processes near the fluid–solid interface, and c) surface kinetics. Changes in the chemistry of the mineralizing solution are unlikely in this case, because the veins are strictly related to the inner parts of the chromite bodies. This fact suggests that the fluid phase precipitated in an essentially closed system. The composition of the fluid, therefore, must have been strongly controlled by the composition of both chromitites and the gabbro sills included in the chromitite pods. Consequently, it is difficult to explain oscillatory zoning by changes in the bulk composition of the fluid.
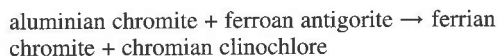
In the opinion of Jamtveit *et al.* (1995) and Ivanova *et al.* (1998), covariation among major elements and similarities among crystals suggest that zoning in garnet is controlled mainly by external forces (flow rates or chemical changes), with only minor participation of surface kinetics. Although the garnet in our suite displays the same type of correlations, we believe that a self-organization process (*e.g.,* Putnis *et al.* 1992) is the most feasible explanation for the oscillatory zoning of the Moa–Baracoa garnet.

A portion of the compositional field of uvarovitic garnet published to date is plotted in Figure 9. It is significant to note that the suite from the Moa–Baracoa massif contains compositions not yet reported in the literature on natural examples of the solid solution uvarovite–grossular, despite the fact that these compositions have already been synthesized (Huckenholz & Knittel 1975).

Kalamarides & Berg (1988) discussed in detail the gaps in this series. On the basis of their own data, experimental work by Huckenholz (1975) and Huckenholz & Knittel (1975), and data supplied by Duke & Bonardi (1982) and Jan *et al.* (1984), they concluded that ugrandite garnet shows complete solid-solution at high temperatures (800–1550°C) and variable pressures (1 bar to 10 kbar). They concluded, also, that a compositional gap exists between uvarovite and grossular at low temperatures. The paragenesis and hydrothermal mode of occurrence at Moa–Baracoa indicate that the garnet crystals formed at relatively low temperature and low pressure. Our data suggest a complete miscibility along the grossular–uvarovite join (*i.e.,* very low level of the andradite component) at low temperatures. The potential of a miscibility gap at greater andradite component cannot be discarded from the data presented. Ganguly (1976) presented a model of the solid solution in the system grossular – uvarovite – andradite. Its calculated spinodal at 400°C does not intersect the uvarovite–grossular join. Because the Moa–Baracoa suite was very likely formed below this temperature, our data do not conflict with this diagram.

These veins formed from a Ca- and Al-bearing hydrothermal fluid. The Al may have been extracted during the replacement of chromite by ferrian chromite (Proenza *et al.* 1997b, Proenza 1998), according to the reaction:

aluminian chromite + ferroan antigorite → ferrian chromite + chromian clinochlore

The activity of Ca in this fluid led to the development of uvarovite, and the development of titanite instead of rutile. The source of Ca-rich fluids in ophiolites is controversial. Mittwede & Schandl (1992) suggested liberation of Ca linked to the phenomenon of serpentinization. In our case, the Ca-rich fluids entered into the system much later than the serpentinization reaction, during low-temperature hydrothermal alteration that replaced serpentine by chlorite. Since the ultrabasic rocks hosting the chromitite pods display a very limited extent of chloritization, the composition of chlorite- and uvarovite-producing fluids seems to be controlled by the composition of the assemblage of chromitites plus the enclosed gabbro sills. The enclosed gabbros could have been an alternative source for Ca. These gabbros were hydrothermally altered, and plagioclase crystals were

converted to prehnite and epidote; clinopyroxene crystals are replaced by fibrous tremolite.

As pointed out above, the uvarovitic garnet as well as the chromitite pods occur in direct association with gabbro sills in the Moa–Baracoa massif (Proenza 1998, Proenza *et al.* 1999). Likewise, the lanthanide patterns (Fig. 11) of gabbros and garnet reflect a similarity in their light rare-earth element contents, with a similar positive Eu anomaly. The positive Eu anomaly in the fresh gabbros is due to Eu^{2+} enrichment in plagioclase owing to the high partition coefficient ($D^{plagioclase/liquid}$) of this element (Harnois *et al.* 1990). As during the early stages of vein infilling, it is uvarovite that is by far the dominant calcium-bearing phase, Eu can also be accommodated in the garnet structure, replacing calcium. On the other hand, the heavy rare-earth enrichment in the garnet is an expression of the general preference of these elements for the garnet structure (*i.e.*, Hanson 1980). The garnet thus seems to have inherited its lanthanide pattern from the gabbro sills during the leaching process that affected both the chromitite bodies and the cross-cutting sills of gabbro.

We conclude, therefore, that the Moa–Baracoa uvarovite was formed by the leaching of Ca from the gabbro sills, and Cr and Al from chromite. The process is associated with low-temperature formation of chlorite and ferrian chromite in the chromitite pods. Extensive crystallization of chlorite and uvarovite is restricted to the chromitite pods. This fact can be attributed to a low mobility of Cr and Al during low-temperature hydrothermal processes operating on ophiolites. These results agree with the low mobility of Cr described in many environments (*i.e.*, Sánchez-Vizcaíno *et al.* 1995, and references therein), and explain the common occurrence of uvarovite in Moa–Baracoa massif. In contrast, uvarovite is absent in Mayarí–Cristal massif. Although this massif underwent the same processes of serpentinization and chloritization as at Moa–Baracoa, gabbro sills or other Ca-rich rocks do not occur. Hence, in the Mayarí–Cristal massif, the supply of Ca to the hydrothermal fluids was lower and, consequently, uvarovite did not form.

REFERENCES

BAMBA, T. (1984): A model illustrating the formative process of the podiform chromite deposits in some alpine orogenic terrains. Syngenesis and epigenesis in the formation of mineral deposits (A. Wauschkuhyn, C. Kluth & R.A. Zimmermann, eds.). Springer-Verlag, Berlin, Germany (507-518).

CHAKRABORTY, K.L. (1968): Mineralogical note on the chrome-chlorite (Kämmererite) and chrome-garnet (uvarovite) from the chromite deposits of Kalrangi, Orissa, India. *Am. Mineral.* **53**, 962-965.

CHRISTIDIS, G.E., ECONOMOU-ELIOPOULOS, M., MARCOPOULOS, T. & LASKOU, M. (1998): An unusual assemblage of high-Ti oxides and ferroan clinochlore along zones of brittle deformation in the Vourinos (Rodiani) ophiolite complex, Greece. *Can. Mineral.* **36**, 1327-1338.

DEER, W.A., HOWIE, R.A. & ZUSSMAN, J. (1992): *Rock-Forming Minerals.* **1A**. *Orthosilicates* (second ed.). Longman, London, U.K.

DUKE, J.M & BONARDI, M. (1982): Chromian andradite from Reaume Township, Ontario. *Can. Mineral.* **20**, 49-53.

DUNN, P.J. (1978): On the composition of some Canadian green garnets. *Can. Mineral.* **16**, 205-206.

FLINT, D.E., DE ALBEAR, J.F. & GUILD, P.W. (1948): Geology and chromite deposits of the Camagüey district, Camagüey Province, Cuba. *U.S. Geol. Surv., Bull.* **954-B**, 39-63.

GANGULY, J. (1976): The energetics of natural garnet solid solution. II- Mixing of the calcium silicate end-members. *Contrib. Mineral. Petrol.* **55**, 81-90.

GRAHAM, I.T., FRANKLIN, B.J. & MARSHALL, B. (1996): Chemistry and mineralogy of podiform chromitite deposits, southern NSW, Australia: a guide to their origin and evolution. *Mineral. Petrol.* **57**, 129-150.

GUILD, P.W. (1947): Petrology and structure of the Moa chromite district, Oriente province, Cuba. *Trans. Am. Geophys. Union* **28**, 218-246.

HANSON, G.N. (1980): Rare earth elements in petrogenetic studies of igneous systems. *Annu. Rev. Earth Planet. Sci.* **8**, 371-406.

HARNOIS, L., TROTTIER, J. & MORENCY, M. (1990): Rare earth element geochemistry of Thetford Mines ophiolitic complex, northern Appalachians, Canada. *Contrib. Mineral. Petrol.* **105**, 433-445.

HEY, M.H. (1954): A new revision of the chlorite. *Mineral. Mag.* **30**, 277-292.

HILLIER, S. & VELDE, B. (1991): Octahedral occupancy and the chemical composition of diagenetic (low-temperature) chlorites. *Clay Mineral.* **26**, 149-168.

HUCKENHOLZ, H.G. (1975): Uvarovite stability in the $CaSiO_3$–Cr_2O_3 join up to 10 kbar. *Neues Jahrb. Mineral., Monatsh.*, 337-360.

_____ & KNITTEL, D. (1975): Uvarovite: stability of uvarovite–grossularite solid solution at low pressure. *Contrib. Mineral. Petrol.* **49**, 211-232.

ITURRALDE-VINENT, M.A. (1996): Ofiolitas y arcos volcánicos de Cuba. *IGCP Project 364, Spec. Contrib.* **1**.

IVANOVA, T.I., SHTUKENBERG, A.G., PUNIN, YU.O., FRANK-KAMENETSKAYA, O.V. & SOKOLOV, P.B. (1998): On the complex zonality in grandite garnets and implications. *Mineral. Mag.* **62**, 857- 868.

JAMTVEIT, B., RAGNARSDOTTIR, K.V. & WOOD, B.J. (1995): On the origin of zoned grossular–andradite garnets in hydrothermal systems. *Eur. J. Mineral.* **7**, 1399-1410.

JAN, M.Q., WINDLEY, B.F. & WILSON R.N. (1984): Chromian andradite and olivine–chromite relations in a chromitite layer from the Jijal complex, northwestern Pakistan. *Can. Mineral.* **22**, 341- 345.

KALAMARIDES, R.I. & BERG, J.H. (1988): Coexisting Cr-rich and Cr-poor garnet from a calc-silicate gneiss, Labrador. *Can. Mineral.* **26**, 335-342.

KENAREV, V.V. (1966): Características mineralógicas del yacimiento Potosí, Cuba. *Revista Tecnológica* **4**, 3-6.

KRANIDIOTIS, P. & MACLEAN, W.H. (1987): Systematics of chlorite alteration at the Phelps Dodge massive sulphide deposit, Matagami, Quebec. *Econ. Geol.* **82**, 1898-1911.

LEBLANC, M. & NICOLAS, A. (1992): Ophiolitic chromites. *Int. Geol. Rev.* **34**, 653- 686.

_____ & VIOLETTE, J.F. (1983): Distribution of aluminium-rich and chromium-rich chromite pods in ophiolite peridotites. *Econ. Geol.* **78**, 293-301.

LEWIS, J.F., MUÑOZ, J.N., PENG, G., CAMPOS, M., QUINTAS, F. (1994): Mineralogy of silicate and chrome-spinel phase in the ophiolite rock and chromite deposits of the Moa–Baracoa area. *Resúmenes del Segundo Congreso Cubano de Geología (Santiago de Cuba)*, 108 (abstr.).

LÓPEZ SÁNCHEZ-VIZCAÍNO, V., FRANZ, G. & GÓMEZ-PUGNAIRE, M.T. (1995): The behavior of chromium during metamorphism of carbonate rocks from the Nevado–Filábride Complex, Betic Cordilleras, Spain. *Can. Mineral.* **33**, 85-104.

MELCHER, F., GRUM, W., SIMON, G., THALHAMMER, T.V. & STUMPFL, E.F. (1997): Petrogenesis of the Ophiolitic giant chromite deposits of Kempirsai, Kazakhstan: a study of solid and fluid inclusions in chromite. *J. Petrol.* **38**, 1419-1458.

MEYER, H.O.A. & BOYD, F.R. (1972): Composition and origin of crystalline inclusions in natural diamonds. *Geochim. Cosmochim. Acta* **36**, 1255-1273.

MITTWEDE, S.K. & SCHANDL, E.S. (1992): Rodingites from the southern Appalachian Piedmont, South Carolina, USA. *Eur. J. Mineral.* **4**, 7-16.

MOGESSIE, A. & RAMMLMAIR, D. (1994): Occurrence of zoned uvarovite–grossular garnet in a rodingite from the Vumba schist belt, Botswana, Africa: implications for the origin of rodingites. *Mineral. Mag.* **58**, 375-386.

MURASHKO, V.I. & LAVANDERO, R.M. (1989): Chromite in the hyperbasite belt of Cuba. *Int. Geol. Rev.* **31**, 90-99.

PAN, YUANMING & FLEET, M.E. (1989): Cr-rich calc-silicates from the Hemlo area, Ontario. *Can. Mineral.* **27**, 565-577.

PINET, M. & SCHMIDT, D.C. (1993): La microspéctrometrie Raman des grenats $X_3Y_2Z_3O_{12}$. I. La série calcique naturelle ouvarovite – grossulaire – andradite. *Schweiz. Mineral. Petrogr. Mitt.* **73**, 21-40.

PROENZA, J. (1998): *Mineralizaciones de cromita en la faja ofiolítica Mayarí–Baracoa (Cuba). Ejemplo del yacimiento Mercedita.* Ph.D. thesis, Univ. of Barcelona, Barcelona, Spain.

_____, GERVILLA, F. & MELGAREJO, J.C. (1997a): Compositional variations of podiform chromitites among different mining districts in the Mayarí–Baracoa Ophiolitic Belt (eastern Cuba). *In* Mineral Deposits: Research and Exploration. Where Do they Meet? (H. Papunen, ed.). Balkema, Dordrecht, The Netherlands (487-490).

_____, _____, _____ & BODINIER, J.L. (1999): Al-rich and Cr-rich chromitites from the Mayarí–Baracoa ophiolitic belt (eastern Cuba): consequence of interaction between volatile-rich melt and peridotite in suprasubduction mantle. *Econ. Geol.* **94**, 547-566.

_____ & MELGAREJO, J.C. (1996): Granates de la serie grosularia–uvarovita en cromititas podiformes del yacimiento Mercedita (Cuba). *Geogaceta* **20**, 1517-1519.

_____, _____ & GERVILLA, F. (1997b): Proceso de alteración a ferricromita en Cr-espinelas del yacimiento Mercedita (Cinturón ofiolítico Mayarí-Baracoa, Cuba). *Bol. Soc. Española Mineral.* **20A**, 29-30.

PUTNIS, A., FERNÁNDEZ-DÍAZ, L. & PRIETO, M. (1992): Experimentally produced oscillatory zoning in the $(Ba,Sr)SO_4$ solid solution. *Nature* **358**, 743-745.

RICKWOOD, P.C. (1968): On recasting analyses of garnet into end-member molecules. *Contrib. Mineral. Petrol.* **18**, 175-198.

RODRIGUEZ-CARVAJAL, J. (1990): FULLPROF: a program for Rietveld refinement and pattern matching analysis. *Satellite Meeting on Powder Diffraction of the XV Congress of the IUCr (Toulouse)*, 127.

SHORE, M. & FOWLER, A.D. (1996): Oscillatory zoning in minerals: a common phenomenon. *Can. Mineral.* **34**, 1111-1126.

SOBOLEV, N.V., LAVRENT'EV, Y.G., POKHILENKO, N.P. & USOVA, L.V. (1973): Chrome-rich garnets from the kimberlites of Yakutia and their parageneses. *Contrib. Mineral. Petrol.* **40**, 39-52.

THAYER, P.T. (1942): Chrome resources of Cuba. *U.S. Geol. Surv., Bull.* **93-A**, 1-74.

VON KNORRING, O., CONDLIFFE, E. & TONG, Y.L. (1986): Some mineralogical and geochemical aspects of chromium-bearing skarn minerals from northern Karelia, Finland. *Bull. Geol. Soc. Finland* **58**, 277-292.

WAN, H.M. & YEH, C.L. (1984): Uvarovite and grossular from the Fengtien nephrite deposits, eastern Taiwan. *Mineral. Mag.* **48**, 31-37.

WADGE, G., DRAPER, G. & LEWIS, J.F. (1984): Ophiolites of the northern Caribbean: a reappraisal of their roles in the evolution of the Caribbean plate boundary. *In* Ophiolites and Oceanic Lithosphere (I.G. Gass, S.J. Lippard & A.W. Shelton, eds.). *Geol. Soc., Spec. Publ.* **13**, 367-380.